



A conceptual investigation for the simultaneous production of gasoline and ammonia in thermally coupled reactors

Mahdi Shakeri, Davood Iranshahi*, Abbas Naderifar

Department of Chemical Engineering, Amirkabir University of Technology (Tehran Polytechnic), No. 424, Hafez Avenue, Tehran 15914, Iran

ARTICLE INFO

Keywords:

Naphtha reforming process
Ammonia synthesis process
Thermally coupled reactor
Aromatic production
Nitrogen conversion

ABSTRACT

In recent years, there have been many efforts to improve the catalytic naphtha reforming, due to the importance of this process in the industry. In this research, simultaneous production of gasoline and ammonia in the thermally coupled reactor is studied theoretically. It is considered that the naphtha reforming process as the endothermic reaction takes place in the shell side of the reactor and ammonia synthesis process as the exothermic reaction takes place in the tube side of the reactor. This configuration leads to an increase in thermal efficiency and reduces operational costs due to the elimination of interstage heaters for catalytic naphtha reforming and reducing of thermal load of condensers for ammonia synthesis unit. In the current research, the results of this new configuration have been compared with results of the conventional naphtha reactors. Obtained results of simulation show an acceptable increase in production yield of the aromatics in reformate compared to the conventional naphtha reforming reactors. On the other hand, the conversion of nitrogen is reduced compared to the conventional ammonia synthesis process slightly. The effect of parameters such as the inlet temperature of the endothermic side, the inlet molar flow rate of the exothermic side, number of tubes and hydrogen to hydrocarbon molar ratio in the naphtha feed on the system performance have been investigated. As well as, some adjustable parameters have been optimized with genetic algorithm method to determine the best solution for this suggested system.

1. Introduction

The feed of the naphtha reforming process (naphtha) contains many hydrocarbons with a low octane number [1]. The task of this unit is to increase the octane number of the final product (reformate) by reactions such as dehydrogenation and hydrocracking [2]. Some kinetic models that explain catalytic reforming have been reported by researchers, which have different degrees of completeness [3–5]. The simplest model presented by Smith [6]. He suggested that this process consists of four main reactions between three pseudo-components containing paraffins, naphthenes and aromatics.

Many researchers studied the modeling and simulating of the catalytic naphtha reactor. For instance, Padmavathi and Chaudhuri [7] investigated the modeling of the reactors of an industrial plant. Gynazova et al. [8] suggested a new approach for mathematical modeling of a continuous catalytic regenerative (CCR) reforming process. Le et al. [9] simulated a semi-regenerative naphtha reformer considering deactivation of the catalyst.

In recent years, have been seen many efforts to improve the catalytic reforming performance. The energy saving issue is a priority in this

process. One of the relevant strategies for energy saving is the thermal coupling of catalytic reforming with an exothermic process in the recuperative reactors. Iranshahi et al. proposed the mathematical modeling for naphtha reforming that coupled with hydrogenation of nitrobenzene to aniline [10]. Due to the high heat released in nitrobenzene hydrogenation, Meidanshahi et al. [11] suggested that the hydrodealkylation of toluene should be replaced with this process. Their study results showed that the replacement of conventional reactors with thermally coupled reactors leads to a 21% in the aromatics production rate. After that, Iranshahi et al. [12] investigated the thermal coupling of toluene hydrodealkylation and catalytic naphtha reforming process in the moving reactors (CCR). They applied a complex kinetic model including 32 lumps in their work. The recuperative reactors have also used in the other processes. Elnashaie et al. [13] suggested a novel integrated dehydrogenation-hydrogenation membrane catalytic reactor. Moustafa and Elnashaie [14] modeled an integrated membrane reactor which is composed of dehydrogenation of ethylbenzene to styrene and hydrogenation of benzene to cyclohexane. They achieved a high production yield of styrene due to the hydrogen transfer from dehydrogenation side by the palladium membrane.

* Corresponding author.

E-mail address: iranshahi@aut.ac.ir (D. Iranshahi).

<https://doi.org/10.1016/j.cep.2019.02.009>

Received 30 June 2018; Received in revised form 29 January 2019; Accepted 22 February 2019

Available online 27 February 2019

0255-2701/ © 2019 Elsevier B.V. All rights reserved.

Nomenclature

a_i	The activity of component i
A_C	Cross-section of the reactor (m^2)
C_p	Specific heat capacity ($\text{kJ}/(\text{kmole})(\text{K})$)
d_p	Particle diameter (m)
D_i	Inside diameter (m)
D_o	Outside diameter (m)
E_i	Activation energy for reaction i (kJ/kmole)
f_i	Fugacity of component i (atm)
f_i^0	Reference fugacity of component i (atm)
F_i	The molar flow rate of component i (kmole/h)
h_i	Heat transfer coefficient in the exothermic side ($\text{W}/(\text{m}^2)(\text{K})$)
h_o	Heat transfer coefficient in the endothermic side ($\text{W}/(\text{m}^2)(\text{K})$)
k_2	Reverse rate constant
k_{fi}	Forward rate constant ($\text{kmole}/(\text{h})(\text{kg cat.})(\text{MPa})$) for reaction (1) and ($\text{kmole}/(\text{h})(\text{kg cat.})(\text{MPa}^2)$) for reaction (2) and ($\text{kmole}/(\text{h})(\text{kg cat.})$) for reactions (3) and (4)
k_{fl}	The thermal conductivity of the fluid ($\text{W}/(\text{m})(\text{K})$)
k_W	The thermal conductivity of the reactor wall ($\text{W}/(\text{m})(\text{K})$)
K_a	Equilibrium constant
K_{ei}	Equilibrium constant (MPa^3 for reaction (1) and MPa^{-1} for reaction (2))
M_i	The molecular weight of component i (kg/kmole)
n	Average carbon number for naphtha
P_i	Partial pressure of component i (kPa)
P_t	Total pressure (kPa)
r_i	Reaction rate for reaction i ($\text{kmole}/(\text{h})(\text{kg cat.})$)
R	Universal gas constant ($\text{kJ}/(\text{kmole})(\text{K})$)
R_{NH_3}	Intrinsic rate of reaction ($\text{kmole}/(\text{h})(\text{m}^3)$)
s_a	Specific surface area of catalyst pellet (m^2/kg)

T	Temperature (K)
u	Velocity (m/s)
U	Overall heat transfer coefficient ($\text{W}/(\text{m}^2)(\text{K})$)
X	Conversion of nitrogen
y_i	The mole fraction of component i
z	Axial coordinate of the reactor (m)

Greek letters

ε	The porosity of catalyst bed
	Effectiveness factor
μ	Viscosity ($\text{kg}/(\text{m})(\text{s})$)
ρ	The density of gas phase (kg/m^3)
ρ_b	The density of reactor bulk (kg/m^3)
ϕ_i	Fugacity coefficient of component i

Subscripts

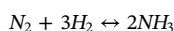
<i>end</i>	Endothermic side
<i>exo</i>	Exothermic side
<i>g</i>	Gas phase
<i>i</i>	Chemical species
<i>j</i>	Sides of the reactor

Abbreviations

<i>FBP</i>	Final boiling point ($^{\circ}\text{C}$)
<i>HC</i>	Hydrocarbons
<i>IBP</i>	Initial boiling point ($^{\circ}\text{C}$)
<i>LHSV</i>	Liquid hourly space velocity (h^{-1})
<i>NOT</i>	Number of tubes
<i>TBP</i>	True boiling point ($^{\circ}\text{C}$)

In this study, it is suggested that the ammonia synthesis process be coupled with the naphtha reforming process. The aim of this novel proposed configuration is the simultaneous production of two important chemical compounds including gasoline and ammonia, as well as reducing energy costs and equipment in both units.

Ammonia is produced based on the nitrogen coming from the air and hydrogen from natural gas at high pressures and high temperatures. This is derived from Haber-Bosch's process along with an iron catalyst as follows [15]:



Ammonia applications as fertilizers, explosives, fibers and synthesizing numerous chemical compounds, are widespread in the industry [15]. Typically, the ammonia synthesis reactor has three adiabatic beds with interstage condensers. Many researchers have simulated and optimized various types of ammonia synthesis reactors [16–20].

Various methods have been proposed for hydrogen production [21,22]. But storage is the most important problem of hydrogen. Since the hydrogen produced by the naphtha unit is immediately consumed in the synthesis of ammonia, there is no storage issue. In this study, it is assumed that the ammonia synthesis reaction occurs in the tube side of the reactor, while the naphtha reforming reactions occur in the shell side of the reactor. The results of this simulation have been compared with both of the conventional processes. The effect of parameters like the inlet temperature of the endothermic side, the inlet molar flow rate of the exothermic side, the number of tubes and hydrogen to hydrocarbon molar ratio in the naphtha feed on the system performance have been studied.

2. Process description

2.1. Industrial catalytic naphtha reforming process

As shown in Fig. 1, the conventional naphtha reforming process is consisted of three adiabatic reactors with interstage heaters to compensate the temperature drop in each bed. Naphtha is mixed with recycle hydrogen. Then the total stream is passed over the commercial Pt-Re/ Al_2O_3 catalyst in beds and the paraffins and naphthenes are converted into aromatics. High-octane reformat is the main product and hydrogen is the by-product. The plant data which applied for the simulation of this process have been presented in Table 1.

2.2. Industrial ammonia synthesis reactor

The reactor of the ammonia synthesis unit is the most important part of this unit [23]. Fig. 2 shows an ammonia synthesis reactor containing two interstage cooling. Table 2 shows the plant data and the operational conditions of the industrial ammonia synthesis reactor. The molar flow rates of components and operating pressure are considered as those reported by Elnashaie et al. [24].

2.3. Integrated of ammonia synthesis beds and naphtha reforming reactors

Fig. 3 shows the schematic diagram of this new coupled reactors. As can be seen, it is suggested that three beds of the ammonia synthesis reactor should be separated. All of the reactors in the industrial naphtha reforming process have been replaced by the thermally coupled reactors containing the ammonia synthesis reaction at the tube side and the naphtha reforming process at the shell side. The heat generated by the

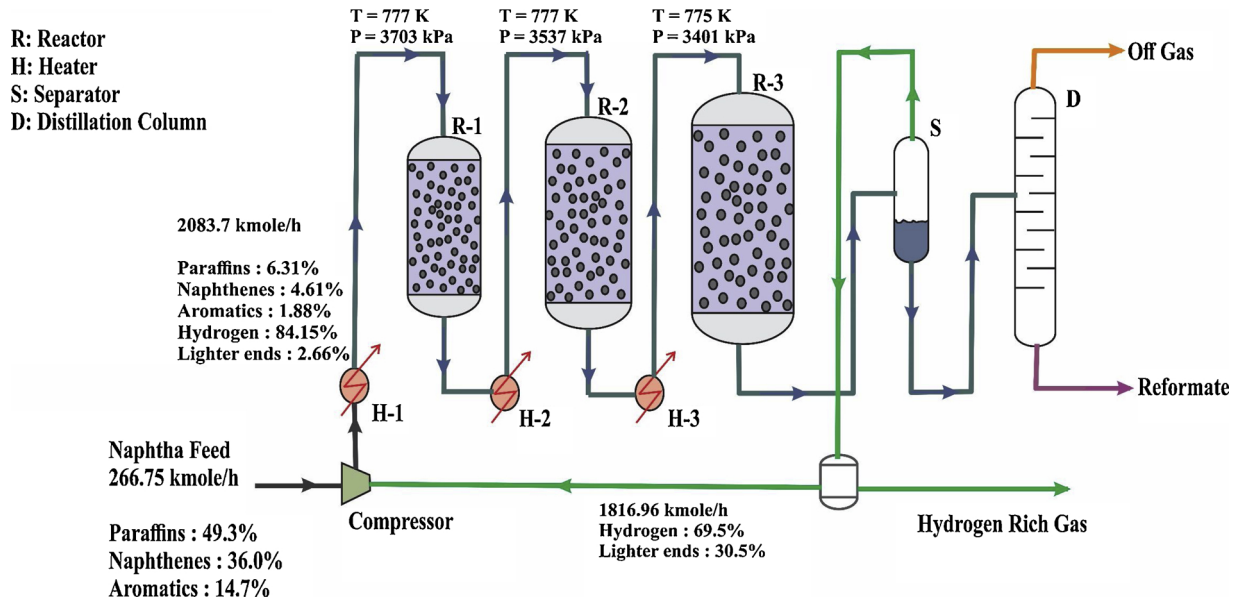


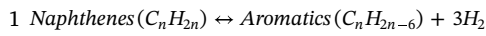
Fig. 1. Schematic of the conventional naphtha reforming process [11].

ammonia synthesis reaction as the exothermic reaction is a good source of heat for the naphtha reforming process as the endothermic reaction. Thus, interstage heaters are eliminated in the naphtha reforming process. In order to increase the production rate of ammonia, the streams of this process are considered to move in the series way. To control the temperature rise in the tube side, interstage condensers are not removed.

3. Reaction kinetics

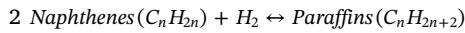
3.1. Endothermic side (Catalytic naphtha reforming process)

Smith [6] suggested that the naphtha is composed of three pseudo-components including paraffins, naphthenes and aromatics and four reactions which take place between these hydrocarbons. These four reactions are as follows:



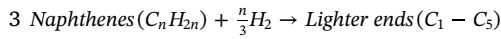
$$\Delta H_1 = 71 \text{ kJ/mole}$$

$$r_1 = \left(\frac{k_{f1}}{K_{e1}} \right) (K_{e1} P_N - P_A P_H^3) \quad (1)$$



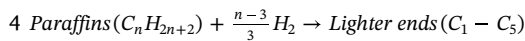
$$\Delta H_2 = -36.9 \text{ kJ/mole}$$

$$r_2 = \left(\frac{k_{f2}}{K_{e2}} \right) (K_{e2} P_N P_H - P_P) \quad (2)$$



$$\Delta H_3 = -51.9 \text{ kJ/mole}$$

$$r_3 = \left(\frac{k_{f3}}{P_i} \right) P_N \quad (3)$$



$$\Delta H_4 = -56.6 \text{ kJ/mole}$$

$$r_4 = \left(\frac{k_{f4}}{P_i} \right) P_P \quad (4)$$

The rate constants (k_f) and the equilibrium constants (K_e) are reported by Rase [25]:

$$k_{f1} = 9.87 \exp \left(23.21 - \frac{E_1}{1.8 T} \right) \quad (5)$$

$$k_{f2} = 9.87 \exp \left(35.98 - \frac{E_2}{1.8 T} \right) \quad (6)$$

$$k_{f3} = k_{f4} = \exp \left(42.97 - \frac{E_3}{1.8 T} \right) \quad (7)$$

$$K_{e1} = 1.04 \times 10^{-3} \exp \left(46.15 - \frac{46045}{1.8 T} \right) \quad (8)$$

Table 1

Specifications of reactors, feed, product and catalyst of the conventional naphtha reforming for fresh catalyst.

Parameter	Numerical value	Unit
Naphtha feed stock	30.41×10^3	kg/h
Reformate	24.66×10^3	kg/h
H ₂ /HC mole ratio	4.74	–
LHSV	1.25	h ⁻¹
Mole percent of hydrogen in recycle	69.5	–
Diameter and length of 1st reactor	1.25, 6.29	m
Diameter and length of 2nd reactor	1.67, 7.13	m
Diameter and length of 3rd reactor	1.98, 7.89	m
Distillation fraction of naphtha feed and reformate		
TBP	Naphtha feed (°C)	Reformate (°C)
IBP	106	44
10%	113	73
30%	119	105
50%	125	123
70%	133	136
90%	144	153
FBP	173	181
Typical properties of catalyst		
Pt	0.3	wt%
Re	0.3	wt%
d _p	1.2	mm
s _a	220	m ² /gr
ρ _b	300	kg/m ³
ε	0.36	–

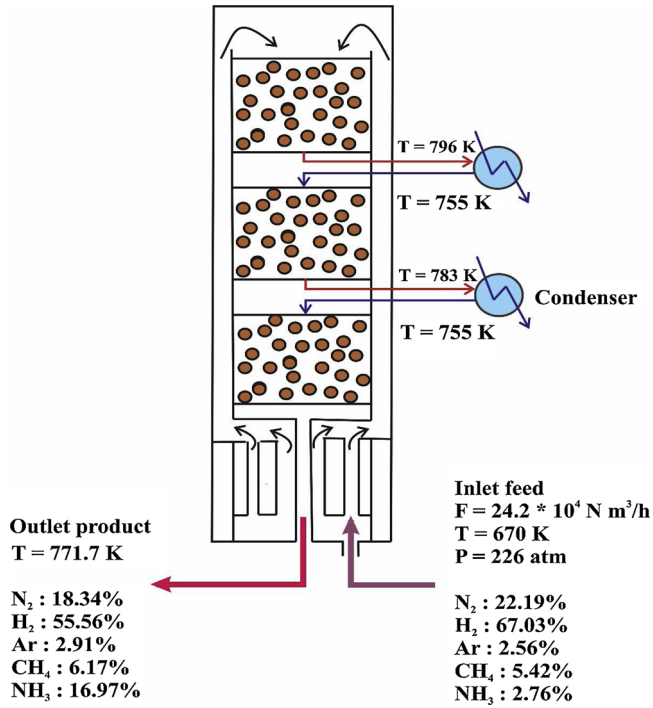


Fig. 2. Schematic of the conventional ammonia synthesis reactor.

Table 2

Specifications of reactors and feed of the conventional ammonia synthesis plant.

Parameter	Numerical value	Unit
Feed molar flow rate	24.216×10^4	N m ³ /h
Feed mole fraction		
N ₂	0.2219	–
H ₂	0.6703	–
CH ₄	0.0542	–
Ar	0.0256	–
NH ₃	0.0276	–
Inlet pressure	226	atm
Number of tubes	100	–
	Inlet temperature (K)	Volume of catalyst bed (m ³)
BED 1	670	4.75
BED 2	755	7.2
BED 3	755	7.8

$$K_{e2} = 9.87 \exp\left(-7.12 + \frac{8000}{1.8T}\right) \quad (9)$$

The activation energies (E) are estimated by [26]:

$$E_1 = 36.3 \text{ kJ/mole}$$

$$E_2 = 58.5 \text{ kJ/mole}$$

$$E_3 = 63.8 \text{ kJ/mole}$$

3.2. Exothermic side (Ammonia synthesis process)

The Temkin equation is applied to obtain the intrinsic rate of the exothermic reaction as follows [27]:

$$R_{NH_3} = k_2 \left[k_a^2 a_{N_2} \left(\frac{a_{H_2}^3}{a_{NH_3}^2} \right)^\alpha - \left(\frac{a_{NH_3}^2}{a_{H_2}^3} \right)^{1-\alpha} \right] \quad (10)$$

α is a constant. In this study, $\alpha = 0.55$ is used. The rate constant of the reverse reaction, k_2 is estimated by the Arrhenius relation as follows:

$$k_2 = 1.7698 \times 10^{15} \exp\left(-\frac{40765 \times 4.184}{RT}\right) \quad (11)$$

K_a is the equilibrium constant and is calculated as follows [24]:

$$\log K_a = -2.691122 \log T - 5.519265 \times 10^{-5} T + 1.848863 \times 10^{-7} T^2 + \frac{2001.6}{T} + 2.6899 \quad (12)$$

In the above equation, T is the temperature in Kelvin. The activity of components, a_i , is obtained as:

$$a_i = \frac{f_i}{f_i^0} \quad (13)$$

where f_i^0 is reference fugacity and be equal to 1 atm. Thus:

$$a_i = f_i = y_i \phi_i P \quad (14)$$

In the above equation y_i is the mole fraction of component i , P is the total pressure in atmosphere and ϕ_i is the fugacity coefficient of component i . The fugacity coefficients of nitrogen, hydrogen and ammonia are given in Appendix A.

4. Mathematical modeling

One dimensional mathematical model has been used in this work. The following assumptions have been exerted in this simulation:

- 1 The model is homogeneous for the naphtha reforming process in the endothermic side and is heterogeneous for the ammonia synthesis process in the exothermic side.
- 2 The coupled reactors are operating at the steady-state condition.
- 3 Due to high pressure in the exothermic side, the pressure drop in this side is assumed to be negligible, while the pressure drop in the endothermic side should be considered.
- 4 There is only heat transfer between the tube and reactor shell, thus there is no heat loss from coupled reactors.

Considering the aforementioned assumptions, the material and heat balance equations for the shell side of the reactor are as follows:

$$\frac{1}{A_C} \frac{dF_{i,end}}{dz} = \rho_b r_{i,end} \quad (15)$$

$$\frac{C_{p,end}^g}{A_C} \frac{d(F_{tot,end} T_{end})}{dz} = \frac{\pi D_o}{A_C} U (T_{exo} - T_{end}) + \rho_b \Sigma r_{i,end} (-\Delta H_{f,i}) \quad (16)$$

The Ergun equation [28] is used for the estimation of the pressure drop in the shell side of the reactor:

$$\frac{dP}{dz} = 150 \frac{(1-\varepsilon)^2 \mu u_g}{\varepsilon^3 d_p^2} + 1.75 \frac{(1-\varepsilon) u_g^2 \rho}{\varepsilon^3 d_p} \quad (17)$$

Material and heat balance equations for the tube side of the reactors are as follows:

$$\frac{1}{A_C} \frac{dF_{i,exo}}{dz} = \eta R_{i,exo} \quad (18)$$

$$\frac{C_{p,exo}^g}{A_C} \frac{d(F_{tot,exo} T_{exo})}{dz} = \frac{-\pi D_i}{A_C} U (T_{exo} - T_{end}) + \eta R_{NH_3} (-\Delta H_r) \quad (19)$$

In Eqs. (17) and (18), is the effectiveness factor that describes the effect of diffusional resistance inside the catalyst particle.

An empirical correlation to calculate the effectiveness factor for the ammonia synthesis process has been derived by Dyson and Simon [27]:

$$\eta = b_0 + b_1 T + b_2 X_{N_2} + b_3 T^2 + b_4 X_{N_2}^2 + b_5 T^3 + b_6 X_{N_2}^3 \quad (20)$$

Where X_{N_2} is the nitrogen conversion and b_i are the coefficients as a function of pressure. These coefficients are tabulated in Table 3 [27]. In Eq. (18), ΔH_r , is the heat of exothermic reaction and has been

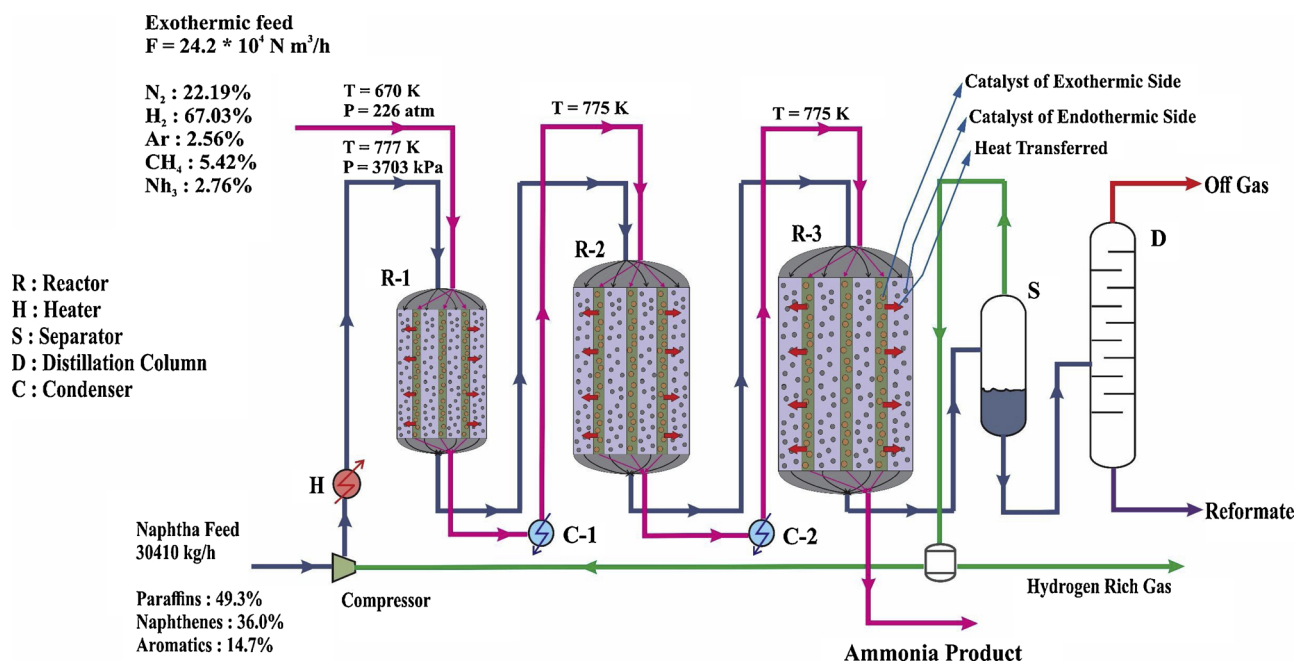


Fig. 3. Schematic of the thermally coupled reactors.

considered in calculations as follows [29]:

$$\Delta H_r = 4.184 \times \left(P \left[0.5426 + \frac{840.609}{T} + \frac{4.5973 \times 10^8}{T^3} \right] - 5.34685 T - \frac{(2.525 \times 10^{-4})}{T^2} + 1.69167 \times 10^{-6} T^3 - 9157.09 \right) \text{kJ/kmole NH}_3 \quad (21)$$

Where P is the pressure in atmosphere and T is the temperature in Kelvin. U is the overall heat transfer coefficient in $\text{W/m}^2\text{K}$. The correlations associated with the calculation of the overall heat transfer coefficient are given in Appendix B.

The boundary conditions are:

$$\text{At } z = 0: F_{i,j} = F_{i,j}^0, T_j = T_j^0, P_j = P_j^0 \quad (22)$$

The mathematical model consists of ordinary differential equations and other auxiliary correlations. These equations have been solved in MATLAB software using the 4th order Runge-Kutta method.

5. Results and discussions

5.1. Model validation

Table 4 presents the simulation and industrial data for the aromatic mole fraction and the temperature at the reactor outlet. As it can be seen, good agreement has been observed between simulated results and industrial data.

5.2. Results

In this study, simulation results have been shown in the diagrams. Fig. 4(a,b) shows the molar flow rate of paraffins, naphthenes, aromatics and hydrogen in the shell side for the conventional and thermally coupled reactors, respectively. As it can be seen in Fig. 4(a), the

consumption rate of the paraffins is higher in the thermally coupled reactors than the conventional reactors in the naphtha reforming process. Fig. 4(a) also shows the molar flow rate of naphthenes versus the length of reactors in the endothermic side. Considering the higher temperature zones in coupled reactors in the naphtha reforming process, the consumption rate of naphthenes is high. Higher consumption rates of paraffins and naphthenes as the main reactants of the naphtha reforming process lead to the higher production rate of aromatics. This fact has been shown in Fig. 5. Aromatics is produced only in the first reaction of the catalytic reforming process. The rate of this reaction has presented for both conventional and coupled reactors in Fig. 5. It is clear that the rate of the first reaction in coupled reactors is higher than the conventional reactors. At the beginning of the first reactor, due to a sudden decrease in the temperature of the endothermic side (Fig. 8), the aromatics production rate is also reduced significantly. The production yield of aromatics in this new configuration is 0.6126, while this value is 0.5608 for the conventional process. Fig. 4 also shows the hydrogen molar flow rate profiles for both conventional and thermally coupled reactors. The molar flow rate of hydrogen at the reactor outlet is approximately the same for both cases. In comparison with the third reactor, the production rate of hydrogen in the first and second reactors is higher. This means that the dehydrogenation reactions are dominant in these reactors.

Fig. 6(a,b) represents the hydrogen and ammonia molar flow rate in the tube side of the thermally coupled reactors, respectively. Heat transfer from the tube side to the shell sides of the coupled reactors reduces the temperature of the ammonia synthesis process. Therefore, the rate of Haber's reaction is reduced and the ammonia in new reactors is produced less than the conventional reactors.

The conversion of nitrogen along the reactors has been presented in Fig. 7. The outlet conversion of nitrogen is 0.2737 for the industrial plant, which has decreased to 0.2676 for this new configuration. In the first reactor, the conversion of nitrogen increases faster than the other

Table 3
Coefficients of Eq. (20) for effectiveness factor calculation.

b_0	b_1	b_2	$b_3 \times 10^5$	b_4	$b_5 \times 10^8$	b_6
-8.2125534	0.03774149	6.190112	-5.354571	-20.86963	2.379142	27.88403

Table 4
Comparison between prediction model and plant data for fresh catalyst.

Reactor No.	Inlet temperature (K)		Inlet pressure (kPa)	Catalyst distribution (wt%)	Input feedstock (mole%)	
1	777		3703	20	Paraffin	49.3
2	777		3537	30	Naphthene	36.0
3	775		3401	50	Aromatic	14.7
No.	Outlet temperature (K)			Aromatic in reformat (mole%)		
	Plant	CNR	TCR	Plant	CNR	TCR
1	722	727.45	777.63	–	–	–
2	753	750.05	790.85	–	–	–
3	770	770.26	774.84	57.70	56.08	61.26

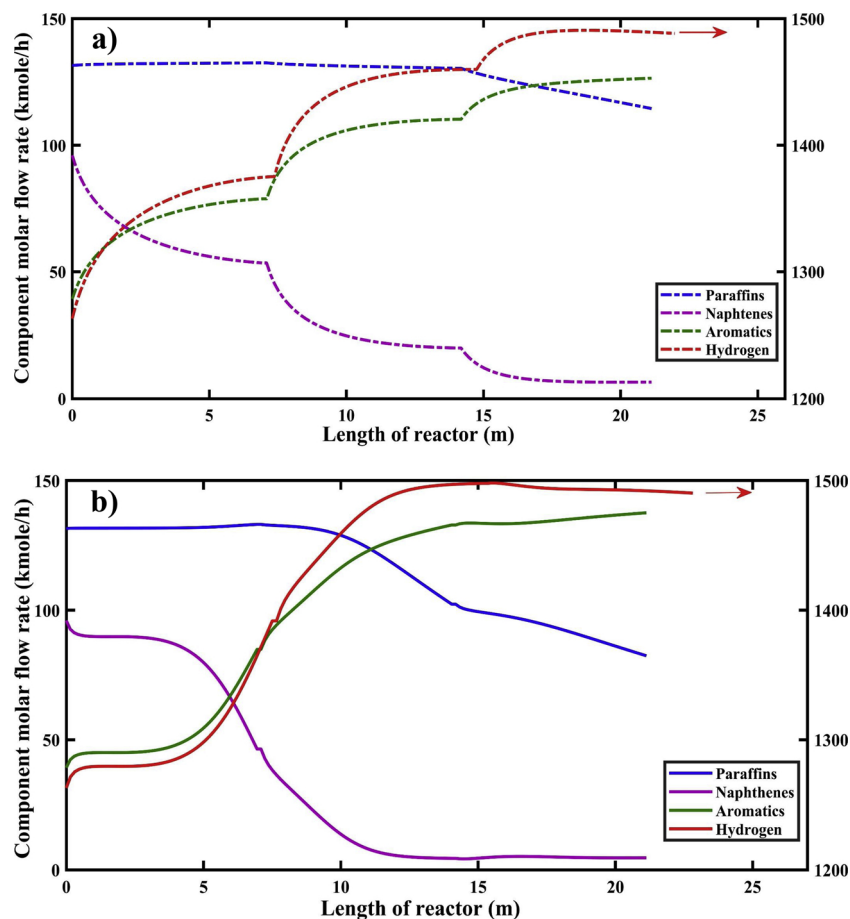


Fig. 4. Component molar flow rate in the naphtha reforming for (a) conventional and (b) coupled reactors.

two reactors for both cases. This means that the forward reaction is dominant in the Haber's process at the first reactor.

Fig. 8(a) shows the temperature profiles of the endothermic and exothermic sides in thermally coupled reactors. In order to justify the temperature profiles, we can use the trend of heat flux diagrams shown in Fig. 8(b). At the entrance of the first reactor, the temperature of the naphtha reforming process is greater than that of the ammonia synthesis process. On the other hand, due to the high reactions rate at the beginning of the naphtha reforming, the heat consumption rate is high (Fig. 8(b)). Therefore, a severe drop in the endothermic temperature occurs to reach a minimum temperature (684.8 K) of 1.56 m from the reactor inlet. From this point to the end of the first reactor, the temperature of the exothermic side is higher than the temperature of the endothermic side, and the heat is transferred from the tube to the shell side. Fig. 8(b) indicates that the transferred heat from the shell side is higher than the consumed heat in this side. Thus, the temperature of the

endothermic side increases (Fig. 8(a)). As it can be seen in Fig. 8(b), the consumed heat in the catalytic reforming is approximately equal to the transferred heat to this process at the end of the third reactor. Consequently, the temperature of the endothermic side must be fixed. This fact has been shown in Fig. 8(b).

Also, the temperature profile of the exothermic side has been presented in Fig. 8(a). In all reactors, the temperature profile raises. This means that the generated heat in the ammonia synthesis reaction is much greater than the transferred heat from the tube side. The generated heat in the first reactor is more than the other two reactors. Consequently, in comparison with the other reactors, the increase in temperature of the tube side in the first reactor is higher. In this configuration, it is suggested to use interstage coolers to control the temperature of the exhaust streams from the exothermic side.

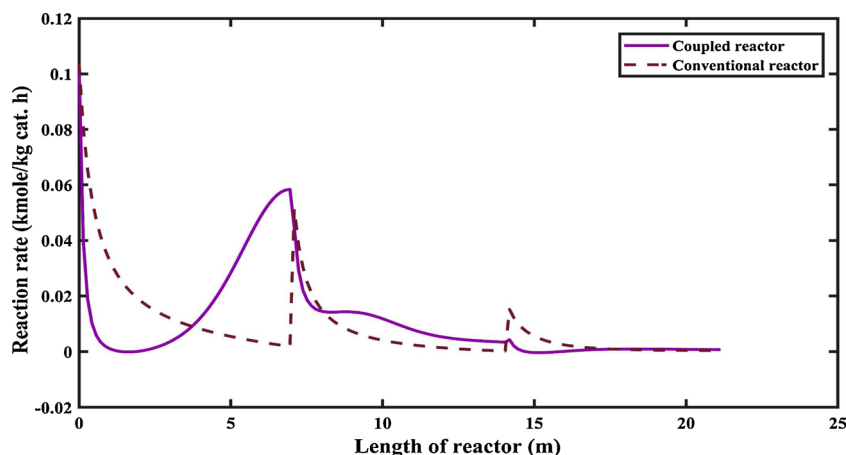


Fig. 5. Rate of first reaction in the naphtha reforming process.

5.3. Analysis of effective parameters

Fig. 9 presents the effect of the inlet temperature of the naphtha feed on the mole fraction of aromatics in the different number of tubes (NOT). According to this figure, initially by increasing the inlet temperature of the naphtha feed the yield of aromatics is decreased to a minimum point. For example, for NOT = 100, the minimum mole fraction of aromatics at reformate is 0.6101. After that, as the temperature increases, the yield of aromatics in reformate increases. The higher number of tubes leads to the higher production rate of

aromatics. This is based on the fact that by increasing the number of tubes, the heat transfer from tubes to the shell is increased and therefore the mole fraction of aromatics in reformate increases. Also, as it can be seen in this figure, as the NOT decreases, the minimum yield of aromatics occurs in higher inlet temperatures of naphtha feed.

The mole fraction of aromatics as the main product of the catalytic naphtha reforming at different inlet molar flow rates of exothermic side and hydrogen to hydrocarbon molar ratios (H_2/HC) in the endothermic side has been shown in Fig. 10. As the initial molar flow rate of the exothermic side increases, the residence time of streams in the tube side

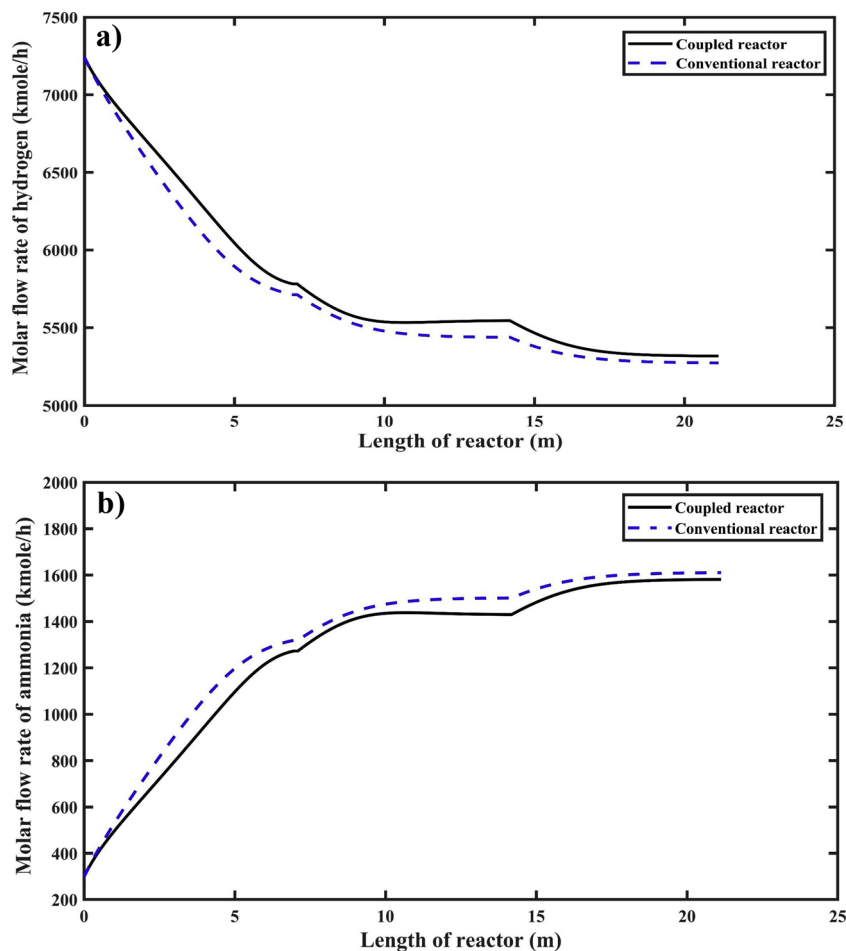


Fig. 6. Molar flow rate of (a) hydrogen and (b) ammonia in the exothermic side.

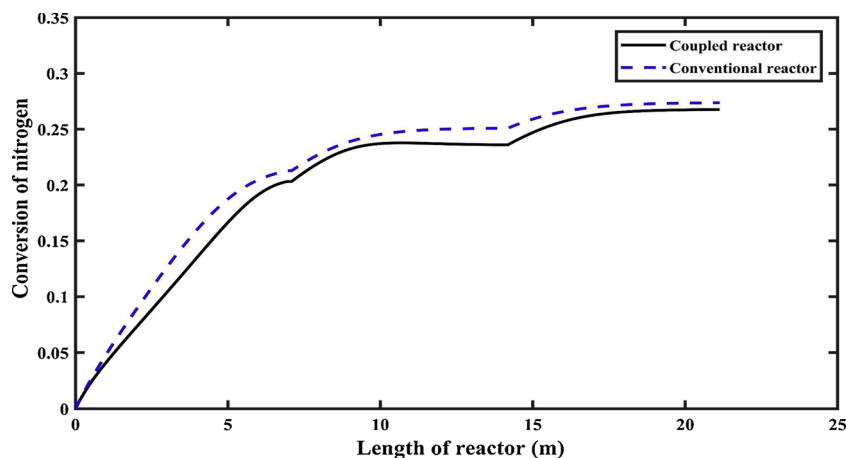


Fig. 7. Conversion of nitrogen in the tube side.

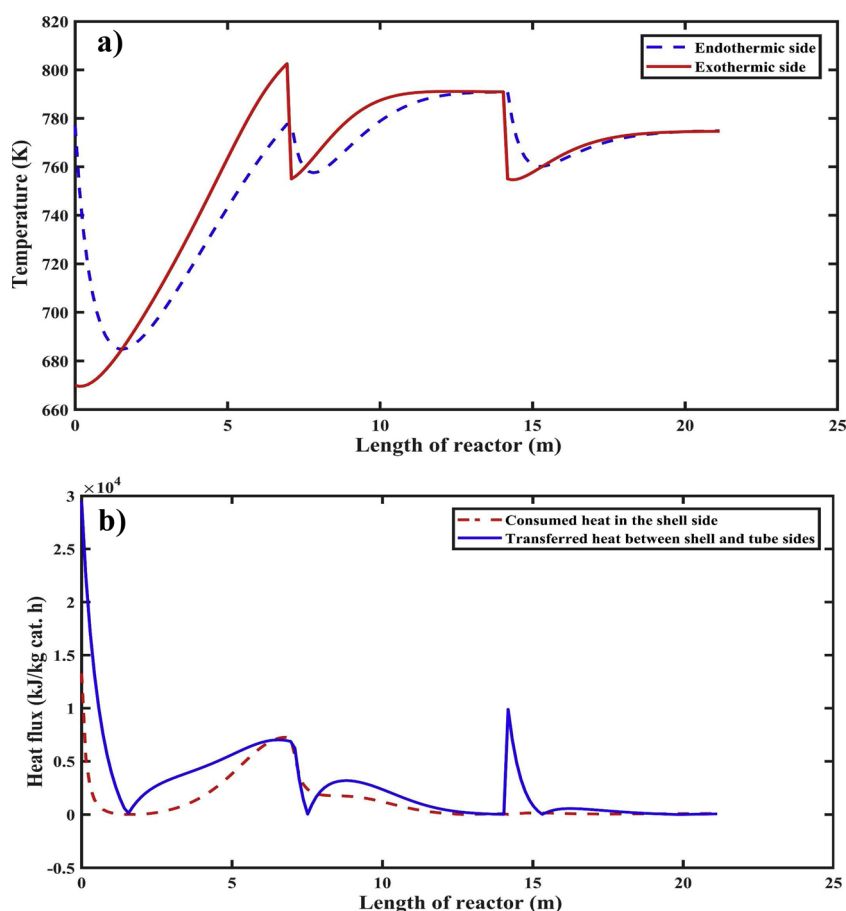


Fig. 8. (a) Temperature profile for endothermic and exothermic sides and (b) the heat flux for the coupled reactors.

decreases. Consequently, the rate of exothermic reaction and thus the heat transfer from the tube side decreases. Therefore, the yield of aromatics at the end of the reactors decreases. Furthermore, at lower hydrogen to hydrocarbon molar ratio, the aromatics molar rate increases. But on the other hand, the deactivation rate of the catalyst in the naphtha reforming process is also increasing.

The effect of the inlet temperature of the exothermic side in the first reactor has been presented in Fig. 11. It is apparent that the higher inlet temperature in ammonia synthesis reaction leads to the higher rate of this reaction. Considering to the high rate of the exothermic reaction, the transferred heat to the naphtha reforming process and thus the mole fraction of aromatics is increased. As it can be seen in this figure, at the

inlet temperature of 690 K for the exothermic side, the aromatics mole fraction can be as high as 0.9; while this value is 0.5608 for the conventional naphtha reforming process.

In this work, the effect of parameters such as the inlet temperature of naphtha feed, the number of tubes, the inlet molar flow rate of the exothermic side and hydrogen to hydrocarbon molar ratio on nitrogen conversion has also been studied in Tables 5 and 6. In the Haber's process, the released heat is much greater than the removed one. For this reason, the effect of combining this process with an endothermic reaction on the production yield of ammonia is very negligible. The conversion of nitrogen at different inlet temperatures of the endothermic side has been tabulated in Table 5 for two number of tubes of

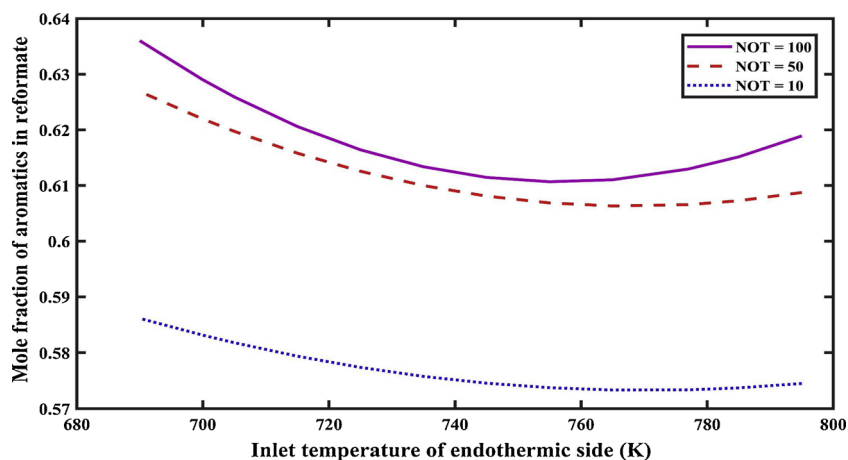


Fig. 9. Mole fraction of aromatics in reformat at different inlet temperatures of naphtha feed and different NOT.

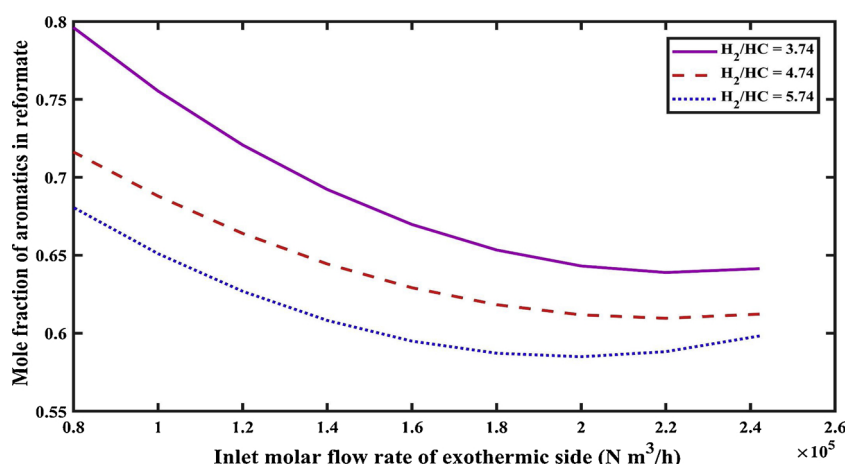


Fig. 10. Mole fraction of aromatics in reformat at different inlet molar flow rates of exothermic side and different H₂/HC.

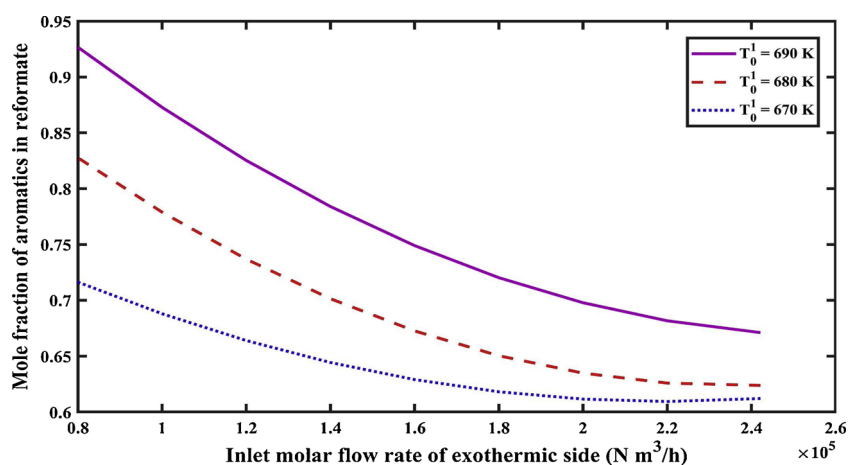


Fig. 11. Mole fraction of aromatics in reformat at different molar flow rates of exothermic side and different inlet temperatures of ammonia feed.

Table 5

Final conversion of nitrogen at different inlet temperatures of naphtha feed and different number of tubes.

Number of tubes	Inlet temperature of naphtha feed (K)			
	795	777	735	700
100	0.2662	0.2676	0.2688	0.2679
50	0.2660	0.2671	0.2677	0.2669

Table 6

Final conversion of nitrogen at different inlet molar flow rates of exothermic side and different hydrogen to hydrocarbon molar ratios.

H ₂ /HC	Inlet molar flow rate of exothermic side × 10 ⁻³ (N m³/h)			
	242.16	120	100	80
4.74	0.2676	0.2691	0.2692	0.2694
3.74	0.2690	0.2692	0.2693	0.2698

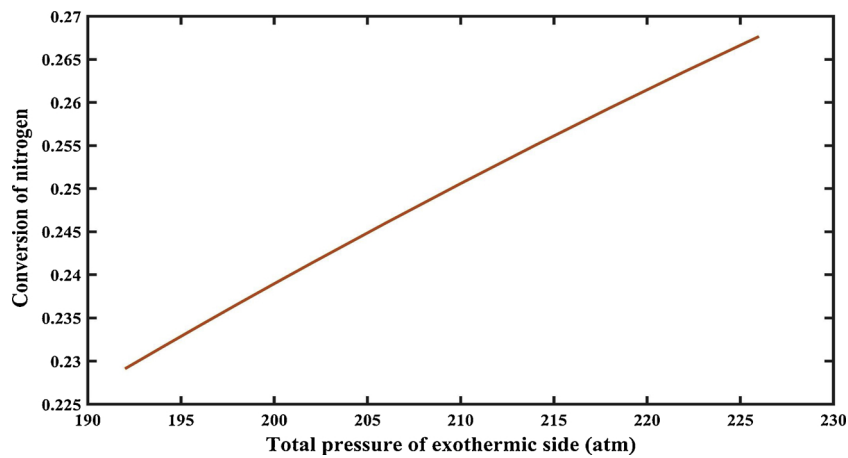


Fig. 12. Nitrogen conversion at the reactor outlet at different total pressures of the exothermic side.

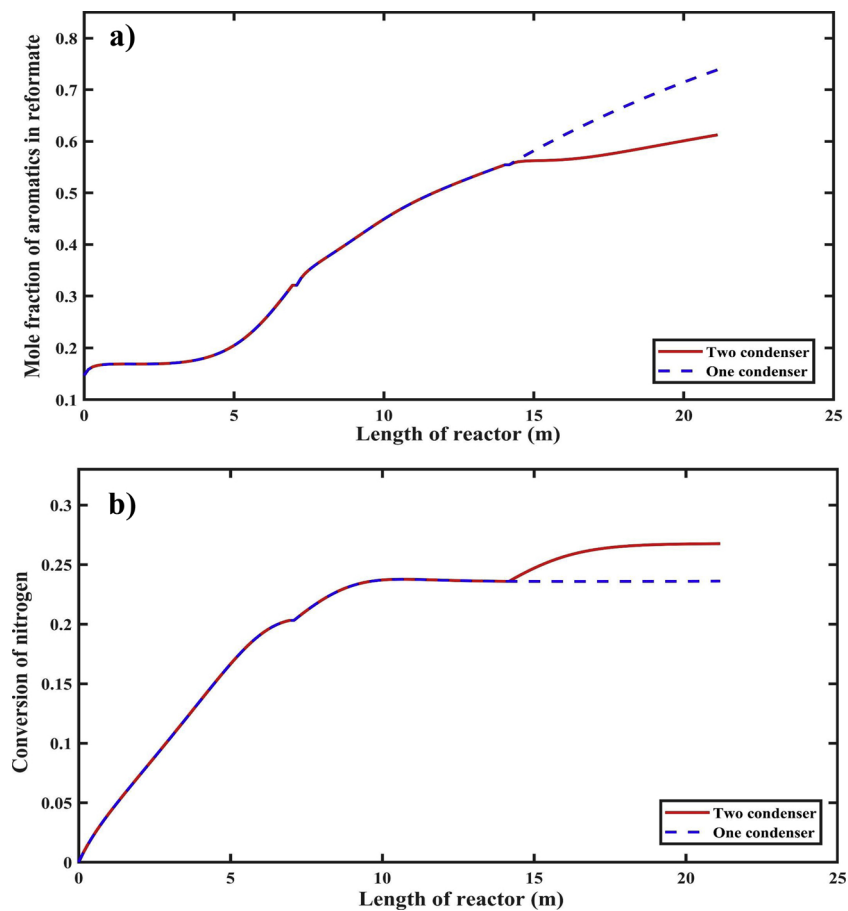


Fig. 13. (a) Mole fraction of aromatics in reformat and (b) Final conversion of nitrogen with/without second condenser.

Table 7

Results of optimization by genetic algorithm.

Parameter	Unit	Min. value	Max. value	Optimum value
Temperature of ammonia feed, T_0^1	K	620	690	667.74
Temperature of naphtha feed, T_0^2	K	700	800	787.25
Inlet molar flow rate of ammonia feed, F_0^1	N m ³ /h	1.0×10^5	3.0×10^5	1.5502×10^5
Molar flow rate of recycle stream in the endothermic side, R	kmole/h	1400	2400	1586.9
Number of tubes in each reactor, NOT	–	1	200	103
Parameter	Non-optimized value		Optimized value	
Aromatics yield, $Yield_{aromatics}$	0.0666		0.0782	
Nitrogen conversion, $X_{nitrogen}$	0.2676		0.2703	

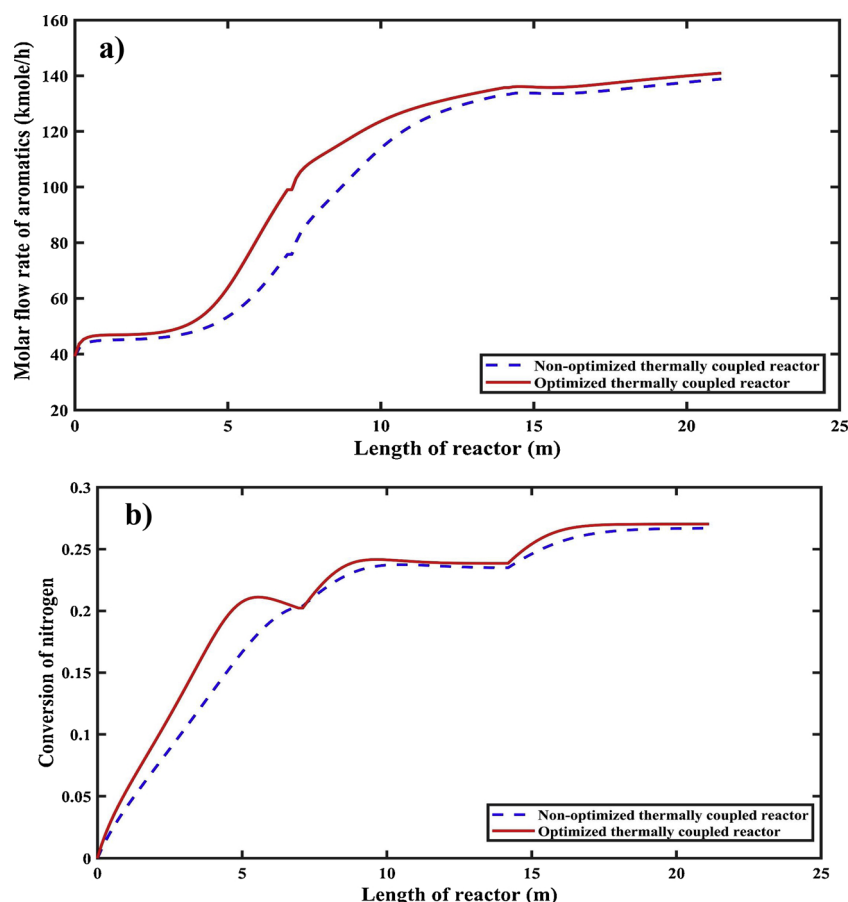


Fig. 14. Result of optimization; (a) aromatic molar flow rate and (b) nitrogen conversion.

100 and 50. Although the effect of the temperature of naphtha feed on the production yield of ammonia is negligible, the maximum conversion of nitrogen is achieved at a specific temperature for any number of tubes. Table 6 represents the values of nitrogen conversion at the tube side for different initial molar flow rates of this side and H_2/HC in the naphtha reforming side. As the molar flow rate of the tube side decreases, the residence time of reactants in the Haber's process increases and thus, the nitrogen conversion increases. However, the slope of increase is very slow. For instance, at H_2/HC of 4.74, the conversion of nitrogen varies from 0.2676 to 0.2694, which its tolerance is about 0.002. As it can be seen in Table 6, by increasing the H_2/HC in the naphtha reforming, the conversion of nitrogen slightly raises.

The effect of the tube side pressure on the nitrogen conversion is sensible. Fig. 12 is evidence of this claim. By decreasing the total pressure of the exothermic side, the Haber's reaction has progressed to the production of nitrogen and its conversion is reduced.

In this new configuration, the effect of elimination of the second condenser has been investigated in Fig. 13(a,b). Fig. 13(a) demonstrates that the mole fraction of aromatics along the reactors before removing the second condenser and after it has been removed. Removing the second condenser leads to a reduction in the operating costs of the process, as well as an increase in the mole fraction of aromatics in reformat from 0.6126 to 0.7388; while the nitrogen conversion decreases from 0.2676 to 0.2361. This fact has been shown in Fig. 13(b).

6. Process optimization

In this study, the single objective optimization method has been applied to obtain the optimal values of some important parameters for the proposed configuration. Genetic algorithms are simple and flexible and have been used in many engineering problems [30–36]. In order to

optimize a problem by genetic algorithms, it is not necessary to calculate the gradients of the objective functions; however these algorithms converge more slowly than the other optimization methods [37].

The objective function of this optimization is the summation of aromatics production yield in the reforming side and the nitrogen conversion in the ammonia side of thermally coupled reactors. The equation of objective function is as follow:

$$OF = Yield_{aromatics} + X_{nitrogen} \quad (23)$$

The aromatics production yield is calculated by following formula:

$$Yield_{aromatics} = \frac{F_{aromatics}^{out}}{F_{fresh\ naphtha\ feed}} \quad (24)$$

The population size of 20 has been used with crossover fraction of 0.8 and mutation probability of 0.05, and generation of 1000. The decision variables of this optimization solution are the temperatures of naphtha and ammonia feeds, the inlet molar flow rate of ammonia feed, the recycle stream of naphtha feed and the number of tubes of each thermally coupled reactor. The constraints for this optimization are as follows:

$$T_1 < 830\ K \quad (25)$$

$$T_2 < 830\ K \quad (26)$$

$$4 < H_2/HC < 6 \quad (27)$$

Table 7 presents the range of above decision variables and their optimal values. The influence of optimization by means of the genetic algorithm on the performance of the proposed system has been demonstrated in Fig. 14(a,b). The aromatics molar flow rate for both optimized and non-optimized thermally coupled reactors has been presented in Fig. 14(a). The production rate of aromatics in the

optimized thermally coupled reactors is increased by about 1% relative to the non-optimized thermally coupled reactors. As well as, the effect of optimization on the behavior of ammonia synthesis process has been demonstrated in Fig. 14(b). The nitrogen conversion and thus, the production of ammonia is slightly improved by means of the process optimization.

7. Conclusion

In this work, it was suggested that instead of interstage heaters in the catalytic naphtha reforming process, the exothermic synthesis ammonia reaction could be used as a heat source for this process. Therefore, it was considered that shell and tube reactors with multiple tubes were used in the simultaneous production of gasoline and ammonia. The production rate of aromatics as the main product of the catalytic reforming increases. The production yield of the aromatics in this configuration is 0.6126; while this value is 0.5608 for conventional reactors. Due to the heat removal from the tube side, the nitrogen conversion reduces about 0.006, which is not very tangible.

The effect of different design parameters on the system performance was studied. With the increase in the number of tubes in the heat exchanger reactors, the heat transferred to the naphtha reforming process increases, and thus the amount of aromatics production increases. Also, as the inlet molar flow rate of the exothermic side decreases, the production rate of aromatics increases. The results revealed that except pressure, the effect of other parameters on the nitrogen conversion is negligible. With the decrease in the inlet pressure of the tube side, the conversion of nitrogen decreases. Finally, the five design parameters of the system have been optimized by means of genetic algorithm procedure. The yield of aromatics and conversion of nitrogen improve by about 17.5% and 1.0% by means of optimization, respectively.

Appendix A and B. Supplementary data

Supplementary material related to this article can be found, in the online version, at doi:<https://doi.org/10.1016/j.cep.2019.02.009>.

References

- [1] I. Elizalde, J. Ancheyta, Dynamic modeling and simulation of a naphtha catalytic reforming reactor, *Appl. Math. Model.* 39 (2015) 764–775.
- [2] G.J. Antos, A.M. Aitani, *Catalytic Naphtha Reforming, Revised and Expanded*, CRC Press, 2004.
- [3] J. Ancheyta-Juarez, E. Villafuerte-Macías, Experimental validation of a kinetic model for naphtha reforming, *Studies in Surface Science and Catalysis*, Elsevier, 2001, pp. 615–618.
- [4] W. Wei, C.A. Bennett, R. Tanaka, G. Hou, M.T. Klein, Detailed kinetic models for catalytic reforming, *Fuel Process. Technol.* 89 (2008) 344–349.
- [5] M.A. Rodríguez, J. Ancheyta, Detailed description of kinetic and reactor modeling for naphtha catalytic reforming, *Fuel* 90 (2011) 3492–3508.
- [6] R. Smith, Kinetic analysis of naphtha reforming with platinum catalyst, *Chem. Eng. Prog.* 55 (1959) 76–80.
- [7] V.G. Padma, Kumar K. Chaudhuri, Modelling and simulation of commercial catalytic naphtha reformers, *Can. J. Chem. Eng.* 75 (1997) 930–937.
- [8] M.S. Gyngazova, A.V. Kravtsov, E.D. Ivanchina, M.V. Korolenko, N.V. Chekantev, Reactor modeling and simulation of moving-bed catalytic reforming process, *Chem. Eng. J.* 176–177 (2011) 134–143.
- [9] L. Jin, T. Yuejin, L. Liangcai, Modeling and optimization of a semi-regenerative catalytic naphtha reformer, *Proceedings of 2005 IEEE Conference on Control Applications*, 2005. CCA 2005. (2005), pp. 867–872.
- [10] D. Iranshahi, A.M. Bahmanpour, E. Pourazadi, M.R. Rahimpour, Mathematical modeling of a multi-stage naphtha reforming process using novel thermally coupled recuperative reactors to enhance aromatic production, *Int. J. Hydrogen Energy* 35 (2010) 10984–10993.
- [11] V. Meidanshahi, A.M. Bahmanpour, D. Iranshahi, M.R. Rahimpour, Theoretical investigation of aromatics production enhancement in thermal coupling of naphtha reforming and hydrodealkylation of toluene, *Chem. Eng. Process. Process. Intensif.* 50 (2011) 893–903.
- [12] D. Iranshahi, R. Saeedi, K. Azizi, M. Nategh, A novel integrated thermally coupled moving bed reactors for naphtha reforming process with hydrodealkylation of toluene, *Appl. Therm. Eng.* 112 (2017) 1040–1056.
- [13] S.S.E.H. Elnashaie, T. Moustafa, T. Alsoudani, S.S. Elshishini, Modeling and basic characteristics of novel integrated dehydrogenation — hydrogenation membrane catalytic reactors, *Comput. Chem. Eng.* 24 (2000) 1293–1300.
- [14] T.M. Moustafa, S.S.E.H. Elnashaie, Simultaneous production of styrene and cyclohexane in an integrated membrane reactor, *J. Memb. Sci.* 178 (2000) 171–184.
- [15] E.P. Carvalho, C. Borges, D. Andrade, J.Y. Yuan, M.A.S.S. Ravagnani, Modeling and optimization of an ammonia reactor using a penalty-like method, *Appl. Math. Comput.* 237 (2014) 330–339.
- [16] C.P.P. Singh, D.N. Saraf, Simulation of Ammonia synthesis reactors, *Ind. Eng. Chem. Process. Des. Dev.* 18 (1979) 364–370.
- [17] L.D. Gaines, Optimal temperatures for Ammonia synthesis converters, *Ind. Eng. Chem. Process. Des. Dev.* 16 (1977) 381–389.
- [18] S.R. Upreti, K. Deb, Optimal design of an ammonia synthesis reactor using genetic algorithms, *Comput. Chem. Eng.* 21 (1997) 87–92.
- [19] B.V. Babu, R. Angira, Optimal design of an auto-thermal ammonia synthesis reactor, *Comput. Chem. Eng.* 29 (2005) 1041–1045.
- [20] M.E.E. Abashar, Implementation of mathematical and computer modelling to investigate the characteristics of isothermal ammonia fluidized bed catalytic reactors, *Math. Comput. Model.* 37 (2003) 439–456.
- [21] S. Saeidi, F. Fazlollahi, S. Najari, D. Iranshahi, J.J. Klemes, L.L. Baxter, Hydrogen production: perspectives, separation with special emphasis on kinetics of WGS reaction: a state-of-the-art review, *J. Ind. Eng. Chem.* 49 (2017) 1–25.
- [22] J.D. Holladay, J. Hu, D.L. King, Y. Wang, An overview of hydrogen production technologies, *Catal. Today* 139 (2009) 244–260.
- [23] M.J. Azarhoosh, F. Farivar, H. Ale Ebrahim, Simulation and optimization of a horizontal ammonia synthesis reactor using genetic algorithm, *RSC Adv.* 4 (2014) 13419–13429.
- [24] S.S. Elnashaie, M.E. Abashar, A.S. Al-Ubaid, Simulation and optimization of an industrial ammonia reactor, *Ind. Eng. Chem. Res.* 27 (1988) 2015–2022.
- [25] H.F. Rase, *Chemical Reactor Design for Process Plants: Case Studies and Design Data*, Wiley-Interscience, 1977.
- [26] A. Khosravanipour Mostafazadeh, M.R. Rahimpour, A membrane catalytic bed concept for naphtha reforming in the presence of catalyst deactivation, *Chem. Eng. Process. Process. Intensif.* 48 (2009) 683–694.
- [27] D.C. Dyson, J.M. Simon, Kinetic expression with diffusion correction for Ammonia synthesis on industrial catalyst, *Ind. Eng. Chem. Fundam.* 7 (1968) 605–610.
- [28] R.B. Bird, W.E. Stewart, E.N. Lightfoot, *Transport Phenomena*, Wiley, 2007.
- [29] S. Strelzoff, *Technology and Manufacture of Ammonia*, Wiley, 1981.
- [30] Y. He, C.-W. Hui, Genetic algorithm based on heuristic rules for high-constrained large-size single-stage multi-product scheduling with parallel units, *Chem. Eng. Process. Process. Intensif.* 46 (2007) 1175–1191.
- [31] Z. Wang, B. Yang, C. Chen, J. Yuan, L. Wang, Modeling and optimization for the secondary reaction of FCC gasoline based on the fuzzy neural network and genetic algorithm, *Chem. Eng. Process. Process. Intensif.* 46 (2007) 175–180.
- [32] X. Chen, N. Wang, Optimization of short-time gasoline blending scheduling problem with a DNA based hybrid genetic algorithm, *Chem. Eng. Process. Process. Intensif.* 49 (2010) 1076–1083.
- [33] H.R. Shahhosseini, D. Iranshahi, S. Saeidi, E. Pourazadi, J.J. Klemes, Multi-objective optimisation of steam methane reforming considering stoichiometric ratio indicator for methanol production, *J. Clean. Prod.* 180 (2018) 655–665.
- [34] L. Montastruc, C. Azzaro-Pantel, L. Pibouleau, S. Domenech, Use of genetic algorithms and gradient based optimization techniques for calcium phosphate precipitation, *Chem. Eng. Process. Process. Intensif.* 43 (2004) 1289–1298.
- [35] J.M. Nougues, M.D. Grau, L. Puigjaner, Parameter estimation with genetic algorithm in control of fed-batch reactors, *Chem. Eng. Process. Process. Intensif.* 41 (2002) 303–309.
- [36] A. Ponsich, C. Azzaro-Pantel, S. Domenech, L. Pibouleau, Constraint handling strategies in Genetic Algorithms application to optimal batch plant design, *Chem. Eng. Process. Process. Intensif.* 47 (2008) 420–434.
- [37] L. Gosselin, M. Tye-Gingras, F. Mathieu-Potvin, Review of utilization of genetic algorithms in heat transfer problems, *Int. J. Heat Mass Transf.* 52 (2009) 2169–2188.